PNAS RESEARCH ARTICLE | MICROBIOLOGY OPEN ACCESS

Palmitoylation-dependent association with Annexin II directs hepatitis E virus ORF3 sorting into vesicles and quasi-enveloped virions

Xing Liu[a,1], Tianxu Liu[b,1], Zhen Shao[a], Xiaoyan Xiong[a,c], Shuhui Qi[a], Junyong Guan[a], Menghang Wang[a], Yan-Dong Tang[a], Zongdi Feng[d,e], Lin Wang[b,1,2], and Xin Yin[a,1,2]

Affiliations are included on p. 11.

Edited by Xiang-Jin Meng, Virginia Polytechnic Institute and State University, Blacksburg, VA; received September 19, 2024; accepted November 25, 2024

Historically considered to be nonenveloped, hepatitis E virus (HEV), an important zoonotic pathogen, has recently been discovered to egress from infected cells as quasi-enveloped virions. These quasi-enveloped virions circulating in the blood are resistant to neutralizing antibodies, thereby facilitating the stealthy spread of infection. Despite abundant evidence of the essential role of the HEV-encoded ORF3 protein in quasi-enveloped virus formation, the underlying mechanism remains unclear. Here, we demonstrate that the HEV ORF3 protein possesses an inherent capacity for self-secretion and that palmitoylation at two cysteine residues within the ORF3 N-terminal region is essential for its secretion and quasi-enveloped virus formation. We further found that only palmitoylated ORF3 proteins hijacked Annexin II for transport to the cytoskeleton and are then directed into multivesicular bodies through the nSMase-endosomal sorting complexes required for transport-III pathway for secretion. Finally, we show that infection of gerbils with HEV mutants harboring mutations at palmitoylation sites within ORF3 showed no fecal viral shedding but competent replication in the liver. Our study fills a gap in the understanding of the assembly and release of quasi-enveloped virions mediated by ORF3 and offers the potential for designing therapeutic strategies to control HEV infection.

hepatitis E virus | ORF3 vesicle | exosome | quasi-enveloped virus | assembly

Significance

The hepatitis E virus (HEV)-encoded ORF3 protein is essential for HEV infection. However, the mechanism by which ORF3 regulates the formation of quasi-enveloped virions remains unclear. In this study, we report that HEV ORF3 can be self-secreted into vesicles and identify Annexin II (ANXA2) as crucial for efficient ORF3 self-secretion and quasi-enveloped virion formation. ANXA2 binds to palmitoylated ORF3, and mutation of the palmitoylation sites in ORF3 disrupts its association with ANXA2, leading to dissociation between ORF3 and the cytoskeleton. Furthermore, an HEV mutant harboring mutations at palmitoylation sites within ORF3 was unable to efficiently secrete infectious viral particles, both in vitro and in vivo. Our findings provide insight into the egress mechanism of quasi-enveloped virions.

Hepatitis E virus (HEV) belongs to the family *Hepeviridae*. Within this family, the genus *Paslahepevirus* contains the main genotypes that infect humans. As a zoonotic pathogen, HEV infects various species including humans, pigs, wild boars, and deer (1). Although most people infected with HEV show no symptoms, approximately one in 20 individuals can develop liver damage (2). Certain populations, such as individuals with immunosuppression (3) and pregnant women (4), also face an increased risk of chronic hepatitis and a high fatality rate when infected with HEV. Currently, a recombinant hepatitis E vaccine (hecolin) is licensed in China, representing a significant advancement in the prevention of HEV infections (5). However, the therapeutic arsenal is only limited to ribavirin and pegylated interferon-α (pegIFN-α) (6). Therefore, there is an urgent need to develop effective preventive and therapeutic strategies.

The HEV genome comprises a single, positive-strand RNA molecule approximately 7.2 to 7.4 kb in length that encodes at least three viral proteins (7). The polyprotein ORF1 translated from the full-length genome is essential for viral replication. ORF2 and ORF3 are translated from a bicistronic subgenomic RNA, of which the capsid ORF2 protein ($ORF2^C$) is responsible for the formation of icosahedral capsids with T = 3 symmetry (8), whereas the secreted ORF2 protein ($ORF2^S$) acts as a decoy by mimicking the capsid structure or antigenic properties to escape neutralizing antibody-mediated antiviral effects (9). The multifunctional ORF3 protein, consisting of 113 or 114 amino acids, is a functional ion channel that plays a vital role in HEV egress (10). Upon translation, ORF3 is likely to undergo posttranslational modifications such as phosphorylation (11) and palmitoylation (12). Palmitoylation at the N-terminal cysteine residues of ORF3 determines its membrane topology and subcellular localization (12). Interestingly, the N-terminal region of ORF3 has been implicated in its interaction with the cytoskeleton (11). However, the mechanism underlying the palmitoylation of ORF3-mediated viral release remains elusive.

HEV was initially classified as a nonenveloped virus after its discovery in the early 1980s (13). However, recent studies have revealed that HEV exists in a quasi-enveloped form, termed eHEV, in the blood of infected patients or culture fluids of infected cells (14, 15). Compared with nonenveloped virions in feces, these eHEV possess additional components,

The authors declare no competing interest.

This article is a PNAS Direct Submission.

[1]X.L., T.L., L.W., and X.Y. contributed equally to this work.

[2]To whom correspondence may be addressed. Email: lin_wang@pku.edu.cn or yinxin@caas.cn.

This article contains supporting information online at https://www.pnas.org/lookup/suppl/doi:10.1073/pnas.2418751122/-/DCSupplemental.

Published December 30, 2024.

including lipid membranes derived from the internal membrane and the ORF3 protein (16). The presence of ORF3 protein in eHEV underscores its significance in the formation and secretion of these unique viral particles. The ORF3 protein interacts with tumor susceptibility gene 101 (TSG101), a component of the endosomal sorting complex required for transport (ESCRT) machinery to mediate eHEV release through the cellular exosomal pathway (17). Moreover, the involvement of two vacuolar protein-sorting proteins (Vps4A and Vps4B) has been observed in the secretion of eHEV via a multivesicular body (MVB) pathway (17). However, the function of ORF3 in the biogenesis and sorting of eHEV into MVB before egress is not well understood.

Annexin II (ANXA2), a member of the annexin family, plays crucial roles in various cellular processes, including membrane organization, ion channel conductance, and the interaction of the F-actin cytoskeleton with the cellular plasma membrane (18). ANXA2 is utilized by human papillomavirus (HPV) (19) to facilitate viral attachment and penetration. It is also vital for the assembly and maturation of measles virus (20), influenza A virus (IAV) (21), enterovirus 71 (22), and hepatitis C virus (HCV) (23). ANXA2 is also involved in the release stage of classical swine fever virus (24) and bluetongue virus (BTV) (25). Moreover, ANXA2 is found in exosomal vesicles and plays a vital role in exosome formation and release (26). Despite the dependence of eHEV egress on the exosomal pathway, whether ANXA2 is involved in the biogenesis and egress of eHEV, remains unclear.

In this study, we demonstrated that the palmitoylation-dependent interaction with ANXA2 directs HEV ORF3 sorting into vesicles and eHEV formation. In addition to its presence in eHEV, we found that ORF3 can also be self-secreted into vesicles. Palmitoylation of ORF3 is essential for its association with ANXA2 and anchoring to the cytoskeleton. Following cytoskeletal transport, ORF3, along with the captured HEV particles, is sorted into vesicles via the nSMase-ESCRT-III pathway. Finally, we showed that palmitoylated ORF3 plays a key role in HEV fecal shedding and circulation to the extrahepatic tissues in an HEV-infected Mongolian gerbil model. Our study contributes to the understanding of the mechanism of ORF3 secretion and its regulatory functions in eHEV formation and provides valuable insights for the development of therapeutic strategies and design of vaccines against HEV.

Results

Both Membrane-Associated ORF3 and Quasi-Enveloped Virions Are Released from Infected Cells. Previous studies have demonstrated that HEV ORF3 is enclosed in eHEV released from infected cells (17). However, whether all extracellular ORF3 proteins are associated with eHEV remains unclear. To address this question, we used HepG2/C3A cells infected with cell culture-derived HEV Kernow-C1/p6 (genotype 3) as a model and confirmed efficient viral replication by staining for the HEV capsid protein and viral RNA quantification (Fig. 1*A* and *SI Appendix*, Fig. S1*A*). As reported previously (9, 27), both the free ORF2^S and HEV ORF3 proteins were detected in the culture fluids of infected cells (Fig. 1*A*). However, unlike the free ORF2^S protein, which is susceptible to degradation upon proteinase K treatment, the extracellular ORF3 protein remained resistant unless treated with detergent, suggesting lipid membrane cloaking (Fig. 1*B*). To further clarify whether all lipid-coated ORF3 proteins were associated with eHEV, we employed rate-zonal centrifugation to effectively separate different viral components in the supernatants. Consistent with previous reports (9), ORF2^S was predominantly detected in fractions 1 to 2 by both western blotting and commercial HEV antigen ELISA. eHEV containing ORF2^C and viral RNAs were enriched in fractions 12 to 16. Intriguingly, in addition to being found in eHEV, a portion of the ORF3 protein (approximately 31 to 40%) was also detected in fractions 7 to 10 (Fig. 1 *C* and *D*), and these ORF3 proteins were also enveloped within the host membrane (Fig. 1*E* and *SI Appendix*, Fig. S1*B*) but was noninfectious (Fig. 1*F*). These results suggest that HEV infection produces membrane-associated ORF3 in addition to eHEV.

Since not all extracellular ORF3 proteins are associated with eHEV, we hypothesized that HEV ORF3 has an inherent capacity for self-secretion. We generated HepG2/C3A cells stably expressing ORF3 alone, ORF3/ORF2^S, or ORF3/ORF2^C via lentivirus-mediated transduction (*SI Appendix*, Fig. S2*A*). We observed efficient secretion of ORF3 from cells, regardless of the presence of ORF2^C or ORF2^S (Fig. 1*G*), indicating that ORF3 alone is capable of secretion. Consistently, extracellular ORF3 was surrounded by a lipid membrane (*SI Appendix*, Fig. S2 *B–D*). To further confirm that the secretion of HEV ORF3 was not a result of compromised membrane integrity induced by ORF3 expression, we assessed cell viability using the trypan blue exclusion assay and cell counting kit-8 assay (CCK8) and found that membrane integrity was almost complete (*SI Appendix*, Fig. S2 *E–G*). More importantly, enhanced green fluorescent protein (EGFP), a non-secretory protein, was detected in the supernatant when fused with HEV ORF3 (Fig. 1*H*). Taken together, these results unequivocally demonstrate that HEV ORF3 possesses an inherent capacity for self-secretion and that quasi-enveloped virions are likely to be produced during the self-secretion of HEV ORF3.

HEV ORF3 Is Secreted from Cells through the Exosomal Pathway. To further characterize the self-secreted ORF3 protein in vesicles, we utilized differential centrifugation to separate different types of extracellular vesicles (Fig. 2*A*). We found that both HEV ORF3 and the exosome markers, including CD81, CD63, Alix, and TSG101 (28, 29), were detected in the vesicles pelleted at 100,000 × g (Fig. 2*B*). These vesicles had an exosome-like morphology (Fig. 2*C*) and measured approximately 100 to 150 nm in size by nanoparticle tracking analysis (NTA) (Fig. 2*C*). To further clarify the role of exosomal pathways in HEV ORF3 secretion, we treated ORF3-expressing cells with inhibitors that blocked exosome biogenesis. The results showed that GW4869, an inhibitor of nSMase activity, efficiently reduced HEV ORF3 secretion in a dose-dependent manner. In contrast, inhibitors such as manumycin, which targets Ras (30) to inhibit its activity (Ras-GFP) (*SI Appendix*, Fig. S3*A*), and Y27632, which inhibits the phosphorylation of LIM domain kinase 1 (LIMK1) to block the microvesicle secretion pathway (*SI Appendix*, Fig. S3*B*) (31), showed no effect on HEV ORF3 secretion, suggesting that HEV ORF3 secretion relies on the nSMase-dependent ESCRT machinery (Fig. 2*D* and *SI Appendix*, Fig. S3 *C* and *D*). Taken together, these results demonstrate that HEV ORF3 is self-secreted from cells via the exosomal pathway.

ANXA2 Is Essential for the Release of both HEV ORF3-Containing Vesicles and Quasi-Enveloped Virions. To elucidate the mechanisms underlying HEV ORF3 self-secretion, we screened for genes related to the exosomal pathway. We selected 47 potential candidates involved in vesicle biogenesis and conducted siRNA screening using an HEV ORF3 self-secreting cell culture model. Both intracellular and extracellular ORF3 were quantified by western blotting and are shown as relative expression levels normalized to those in scrambled siRNA-transfected cells (Fig. 3*A* and *SI Appendix*, Fig. S4*A*). In line with previous studies (16, 17), we found that the depletion of factors related to the ESCRT

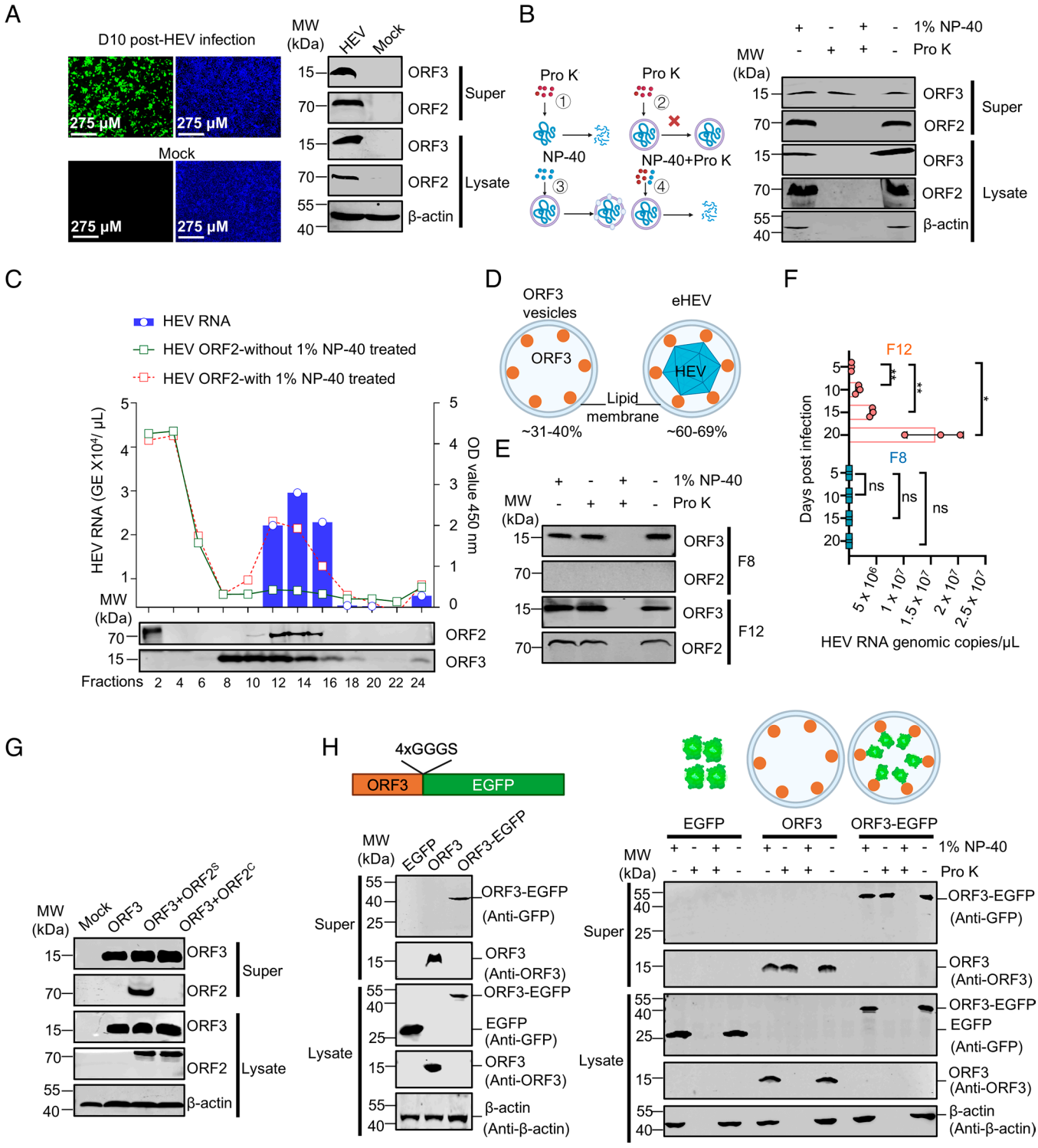

Fig. 1. ORF3 vesicles and quasi-enveloped virions are secreted from HEV-infected cells. (*A*) HepG2/C3A cells were infected with HEV (Kernow-C1/p6, genomic copies/cell = 10,000), and the viral replication was assessed by IFA and western blotting. Representative results from three independent experiments are shown. (*B*) Pipeline for distinguishing the membrane-coated proteins from free proteins. Culture supernatant collected from infected cells was treated with 1% NP-40 and 200 μg/mL proteases. Viral proteins were then detected by western blotting. Representative results from two independent experiments are shown. (*C*) Culture supernatants from HEV-infected cells were separated by sucrose density gradient centrifugation and then analyzed by western blots, qRT-PCR, and indirect ELISA. Representative results from two independent experiments are shown. (*D*) Percentage of ORF3 proteins in fractions 7 to 10 and fractions 11 to 16. (*E*) ORF3 in fractions 8 and 12 were treated with proteinase K in the presence or absence of 1% NP-40, and the degradation of ORF3 and ORF2 proteins was examined by western blotting. The blots are representative of two independent experiments. (*F*) Infectivity of virions in fractions 8 and 12 was determined by infection of HepG2/C3A cells at the same protein level of ORF3, and viral genomic copy numbers were detected by qRT-PCR. Data represent mean ± SD from three independent experiments each in duplicate wells, $*P < 0.05$; $**P < 0.01$; $***P < 0.001$; ns, not significant. (*G*) Detection of intra- and extracellular ORF2 and ORF3 protein expression in HepG2/C3A cells stably expressing ORF3, ORF3/ORF2^S, or ORF3/ORF2^C by western blotting. Blots are representative of two independent experiments. (*H*) HepG2/C3A cells transfected with constructs expressing EGFP, ORF3 alone, or fused ORF3-EGFP with linker of flexible peptide $GGGS_4$. At 36 h posttransfection, intra- and extracellular proteins were detected with indicated antibodies. Culture supernatant and lysates of cells transfected with the construct expressing EGFP, ORF3, or ORF3-EGFP were further subjected to proteinase K protection assay, respectively. The blots are representative of two independent experiments. "Pro K" stands for "proteinase K".

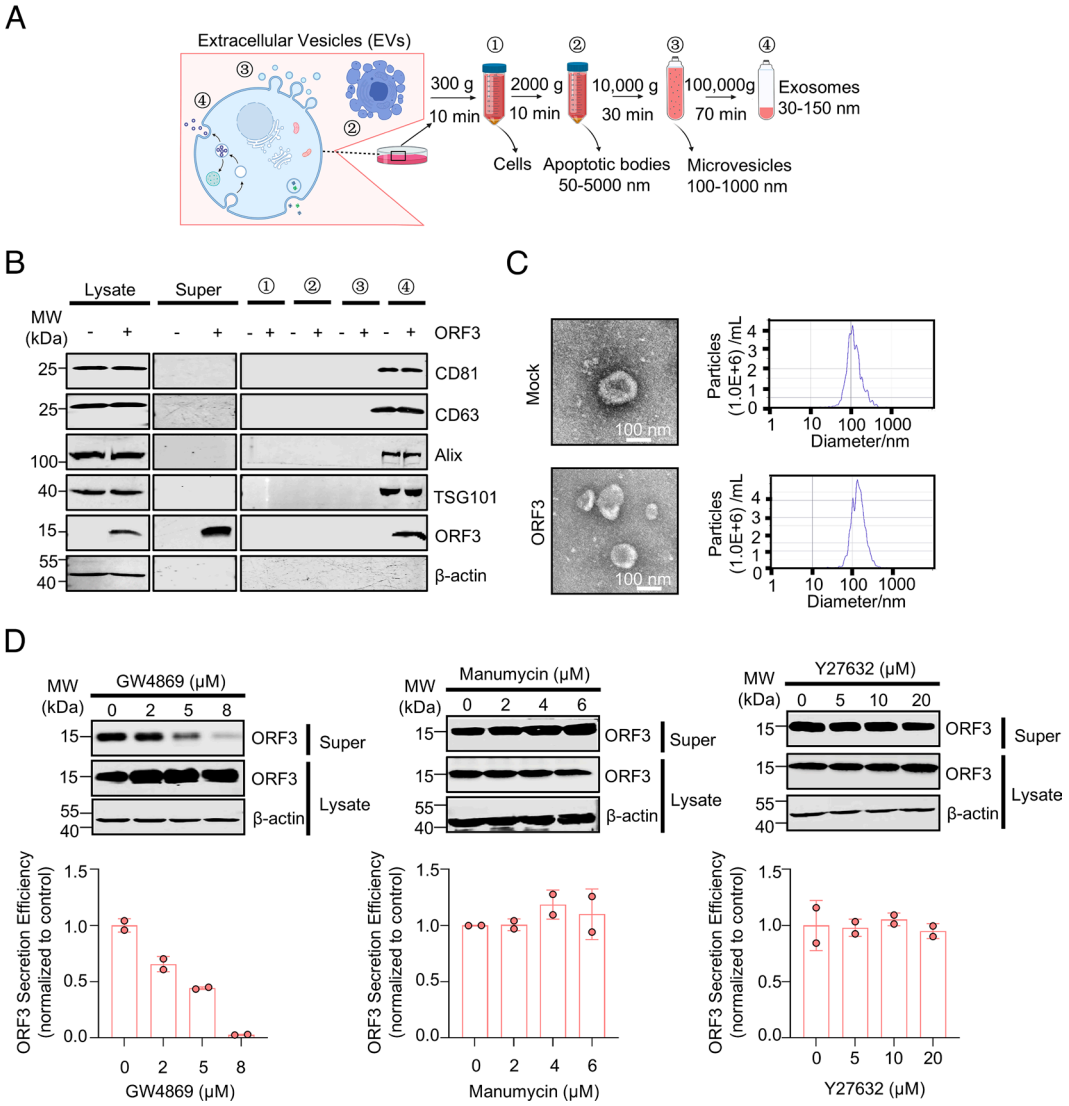

Fig. 2. ORF3 vesicles resemble exosomes and are secreted via the nSMase-ESCRT III pathway. (*A*) Pipeline for the separation of extracellular vesicles by differential centrifugation (Created with BioRender.com). (*B*) Culture supernatant of HepG2/C3A cells stably expressing HEV ORF3 protein was collected and separated by differential centrifugation. The resulting fractions were analyzed by staining with exosome marker proteins (CD81, CD61, Alix, and TSG101) and ORF3. The blots are representative of two independent experiments. (*C*) Electron microscopy observation (*Left*) and NTA (*Right*) of purified vesicles from culture supernatant of HepG2/C3A stably expressing ORF3 or mock cells. (*D*) HepG2/C3A cells stably expressing ORF3 were treated with inhibitors of GW4869, manumycin, or Y27632 at different doses. At 48 h posttreatment, extracellular ORF3 was detected by western blotting. Representative results from two independent experiments are shown.

pathway, such as TSG101, VPS25, HSP90AA1, and CHMP1B, resulted in a significant reduction in ORF3 secretion (Fig. 3 *A* and *B* and *SI Appendix*, Fig. S4 *A* and *B*). Additionally, the knockdown of ANXA2, an important member of the annexin family, was spatially located in the vesicle-bound cytoplasm, nucleus, and on the inner and outer leaflets of the plasma membrane (32), almost entirely halting ORF3 secretion (Fig. 3*C* and *SI Appendix*, Fig. S4*C*), whereas the overexpression of ANXA2 substantially increased extracellular ORF3 levels in a dose-dependent manner (Fig. 3*D*). ANXA2-depletion also resulted in a decrease in ORF3 secretion in infected cells, although viral replication remained unaffected, as evidenced by intracellular viral RNA quantification and viral ORF2 protein evaluation, and $ORF2^S$ secretion in the supernatants (Fig. 3 *E* and *F* and *SI Appendix*, Fig. S5 *A* and *B*). Moreover, the extracellular viral RNA detected in fraction 16 was threefold lower, suggesting that eHEV egress in cells that were depleted of ANXA2, was also impeded by the deficiency of HEV ORF3 self-secretion (Fig. 3*F*). Given the crucial role of ANXA2 in HEV ORF3 secretion, we further explored whether HEV ORF3 specifically exploits ANXA2 for secretion. Our results revealed that in the context of HEV ORF3 expression or HEV infection, elevated ANXA2 levels were detected in the supernatants (Fig. 3*G*). Furthermore, coimmunoprecipitation (Co-IP) assays revealed a specific interaction between ORF3 and ANXA2 (Fig. 3*H*), and confocal imaging showed the colocalization of ORF3 and ANXA2 (Fig. 3*I* and *SI Appendix*, Fig. S5*C*). Collectively, these results underscore the specific role of ANXA2 in mediating HEV ORF3 self-secretion and eHEV formation.

C_{18} and C_{21} at the N-Terminal of HEV ORF3 Are Essential for Binding with ANXA2. To identify the key amino acids within ORF3 responsible for ANXA2 binding, we performed alanine scanning mutagenesis by sequentially introducing five alanine substitutions (Fig. 4*A* and *SI Appendix*, Fig. S6 *A*–*C*). Our results showed that the ORF3 mutant harboring the mutation at $FCLCC_{17\text{-}21}$ significantly reduced its binding ability with ANXA2 (Fig. 4*A*). Further mutagenesis revealed that the amino acids at positions 18 and 21 were essential for binding to ANXA2, as ORF3-C_{18}A/C_{21}A mutant completely lost its binding affinity for ANXA2 (Fig. 4*B*). Additionally, the colocalization signal between

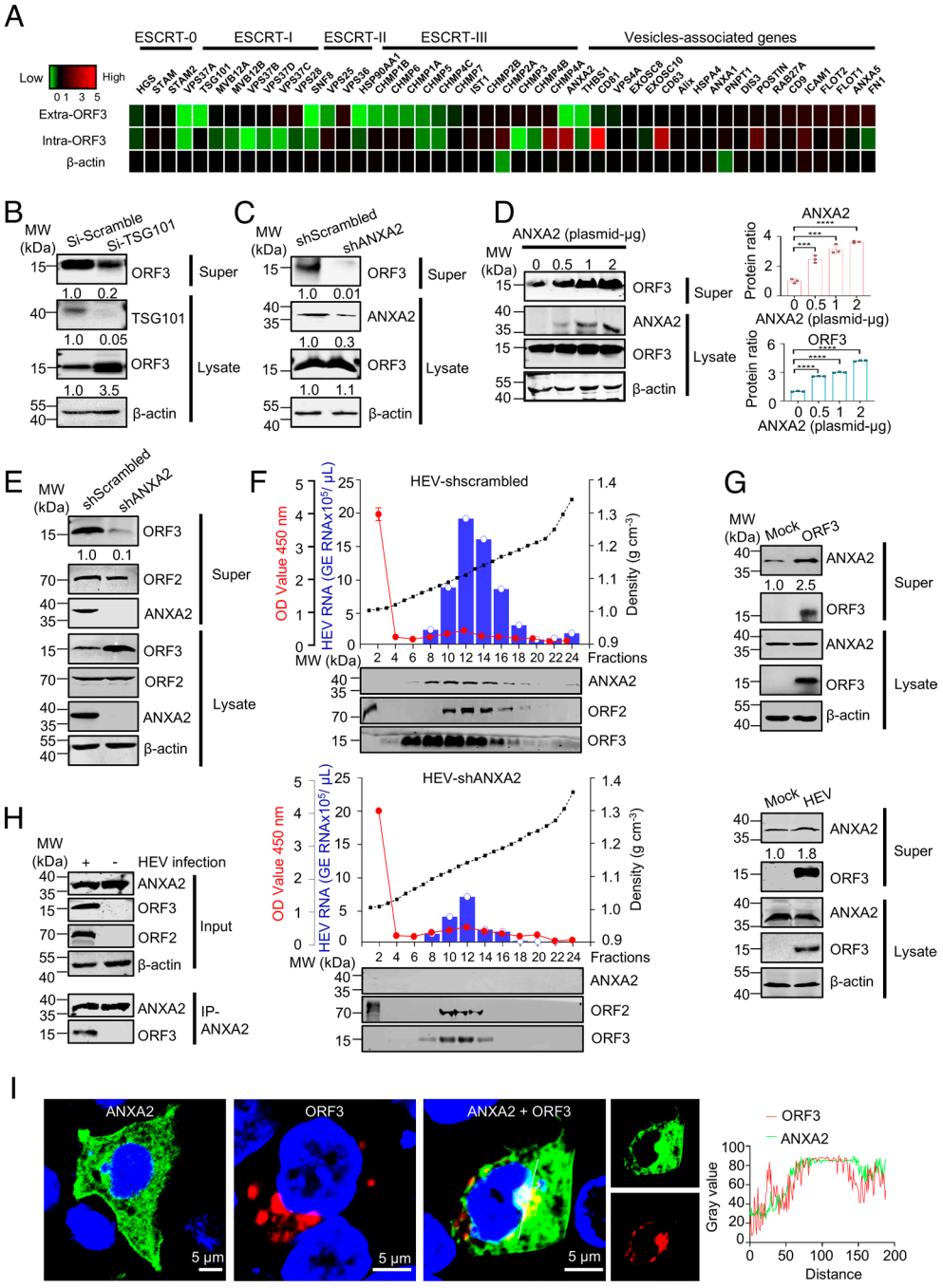

Fig. 3. ORF3 specifically interacts with ANXA2 for the secretion of ORF3 vesicles and quasi-enveloped virions. (*A*) HepG2/C3A cells stably expressing ORF3 were transfected with an arrayed siRNA at 10 pmol. Extra- and intracellular ORF3 were then detected by western blotting at 48 h posttransfection, and the relative expression level was calculated by normalizing to that in cells transfected with scrambled siRNA, and presented as a heatmap. Data represent mean from three independent experiments. (*B*) HepG2/C3A cells stably expressing ORF3 were transfected with siRNA targeting TSG101, and the protein level of TSG101, ORF3, and β-actin in cell lysates, as well as ORF3 in supernatant, were detected by western blotting. The blot is representative of two independent experiments. (*C*) HepG2/C3A cells expressing ORF3 were stably knocked down for ANXA2 using specific shRNA, and extracellular ORF3 protein levels were assessed by western blotting. ANXA2 and ORF3 protein levels were quantified using image analysis. The blot is representative of two independent experiments. (*D*) HepG2/C3A cells were transfected with plasmids expressing ANXA2 at different doses (0, 0.5, 1, or 2 μg/well). At 36 h posttransfection, ANXA2, ORF3, and β-actin in cell lysates, as well as ORF3 in culture supernatant, were analyzed by western blotting. The protein level of ANXA2 or ORF3 was quantified using ImageJ analysis and normalized to control. Data represent mean ± SD from three independent experiments, $*P < 0.05$; $**P < 0.01$; $***P < 0.001$; ns, not significant. (*E*) HepG2/C3A cells depleted of ANXA2 were infected with HEV (genomic copies/cells = 10,000). HEV ORF3, ORF2, and ANXA2 were detected by western blotting and analyzed by ImageJ. β-actin was detected as loading control. The blot is representative of two independent experiments. (*F*) HepG2/C3A [wild-type (WT) or ANXA2 KD] were infected with HEV. At 10 d postinfection, the culture supernatants were separated by sucrose density gradient centrifugation to isolate potential different forms of ORF3 protein and analyzed by western blotting and qRT-PCR. Representative results from two independent experiments are shown. (*G*) Culture supernatant and lysates of HepG2/C3A cells stably expressing ORF3 or HepG2/C3A cells infected with HEV at 10 d postinfection were collected. ANXA2 and ORF3 protein levels were detected and analyzed by western blotting. The blot is representative of two independent experiments. (*H*) HepG2/C3A cells were infected with HEV (genomic copies/cell = 10,000). The cell lysates were collected for coimmunoprecipitation at 10 d postinfection. Representative results from two independent experiments are shown. (*I*) HepG2/C3A cells were transfected with plasmids of pCAGGS-ORF3-mRuby or pANXA2-EGFP-N1 or both. At 36 h posttransfection, cells were fixed by 4% paraformaldehyde, stained with DAPI for nuclei, and observed using confocal microscopy. Confocal images were then captured (63× magnification). 18/20 cells in 10 images exhibited colocalization between ORF3-mRuby and ANXA2-EGFP. Colocalization signals were analyzed by ImageJ.

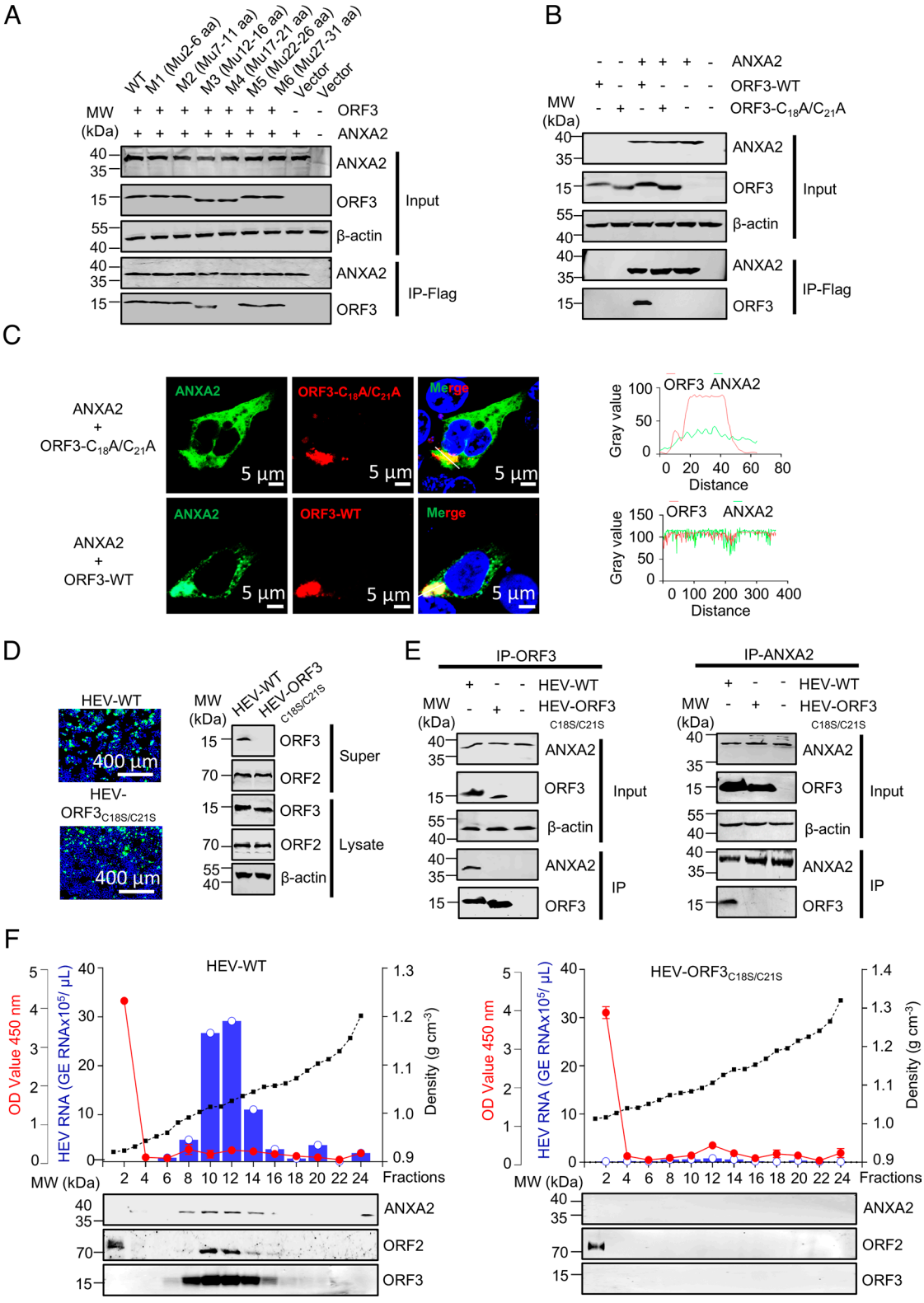

Fig. 4. C_{18} and C_{21} are key amino acids of HEV ORF3 for interacting with ANXA2. A-B. HEK293T cells were transfected with the plasmid pCAGGS-ANXA2-Flag along with either pCAGGS-ORF3-HA or mutated forms of ORF3 using 5× alanine scanning (*A*) or the ORF3-C_{18}A/C_{21}A mutant (*B*). Cell lysates were collected for coimmunoprecipitation assays. Blots are representative of two independent experiments. (*C*) Confocal images showing the colocalization of ORF3-WT (red), ORF3-C_{18}A/C_{21}A (red), and ANXA2 (green). Nuclei were stained with DAPI. Images were captured using a confocal microscope (63×). 20/23 cells in 10 images exhibited colocalization between ORF3-WT and ANXA2, while 1/25 cells in 10 images exhibited colocalization between ORF3-C_{18}A/C_{21}A and ANXA2. Colocalization signals of ORF3 and ANXA2 were analyzed using the ImageJ software. (*D*) HepG2/C3A cells were infected with HEV-WT or a mutant (HEV-ORF3$_{C18S/C21S}$) with 10,000 genomic copies per cell. Viral replication was evaluated by observing HEV ORF2 expression through IFA. Both intracellular and extracellular ORF3 were detected by western blotting and analyzed using the ImageJ software. β-actin was detected as loading control. Representative results from two independent experiments are shown. (*E*) Coimmunoprecipitation with conjugated antibodies against ORF3 or ANXA2 demonstrates the interaction between ORF3 and ANXA2 in infected cells. Blots are representative of two independent experiments. (*F*) Culture supernatants of HEV-infected cells were subjected to rate-zonal centrifugation, and the collected fractions were analyzed using qRT-PCR and western blotting. HEV antigen levels in the culture supernatant were measured using the ELISA. Representative results from two independent experiments are shown.

the ORF3-C_{18}A/C_{21}A mutant and ANXA2 was weakened (Fig. 4*C*). Consequently, self-secretion of ORF3-C_{18}A/C_{21}A was severely impaired (*SI Appendix*, Fig. S6 *D* and *E*). Moreover, when these mutations were introduced into the HEV genome, the HEV mutant carrying C_{18}S/C_{21}S efficiently replicated in HepG2/C3A cells, but ORF3 secretion was completely inhibited (Fig. 4*D*), and the interaction between ORF3 and endogenous ANXA2 was abolished in HEV mutant-infected cells (Fig. 4*E*). Consequently, less HEV $ORF2^C$ or viral RNA was detected in fractions 9 to 14 by western blotting and quantitative RT-PCR, respectively (Fig. 4*F*). Taken together, C_{18} and C_{21} at the N terminus of HEV ORF3 are essential for its binding with ANXA2 and secretion, and HEV mutants lacking the sites essential for ORF3 interaction with ANXA2 were unable to efficiently release ORF3 vesicles and eHEV. These results suggest that ORF3 plays a vital role in the egress of HEV particles by exploiting ANXA2, and ORF3 self-secretion is a prerequisite for effective eHEV release.

Binding with ANXA2 Requires the Palmitoylation of ORF3 at C_{18} and C_{21}. Previous studies identified HEV ORF3 as a palmitoylated protein (12). GPS-Palm analysis showed that C_{18} and C_{21} were potential palmitoylation sites with high area under the curve scores. Palmitoylated proteins were detected in the cleaved bound fraction (cBF) using a resin-assisted capture method. We observed the presence of the HEV ORF3 protein in the input fraction, cBF, and preserved unbound fraction, but not in the cleaved unbound fraction (cUF) or preserved bound fraction (Fig. 5 *A* and *B*). As a negative control, nonpalmitoylated HEV ORF2 was detected in the cUF rather than in the cBF (*SI Appendix*, Fig. S7*A*), confirming that palmitoylation of HEV ORF3 is specific. Intriguingly, treatment with 2-bromopalmitate (2-BP), a potent palmitoylation inhibitor (12), altered the distribution pattern of HEV ORF3 in the fractions, with HEV ORF3 detected in the cUF (Fig. 5 *A* and *B*), and led to the observation of one ORF3 band with a lower molecular weight (Fig. 5 *A* and *B* and *SI Appendix*, Fig. S7*B*), indicating that 2-BP blocked the palmitoylation of HEV ORF3. More importantly, the ORF3-C_{18}A/C_{21}A mutant exhibited lower levels of palmitoylation, as indicated by the substantial amount of ORF3 protein detected in the cUF. This result suggested that C_{18} and C_{21} are the key amino acids involved in ORF3 palmitoylation (Fig. 5 *A* and *B*). To further determine whether palmitoylation of ORF3 is required for binding to ANXA2, we compared the binding efficiency of ORF3 and ANXA2 with or without 2-BP treatment (Fig. 5*C*). Treatment with 2-BP in cells infected with HEV led to the detection of the nonpalmitoylated ORF3 form with a lower molecular weight, as shown above. Only the palmitoylated ORF3 form with a higher molecular weight was detected in immunoprecipitated samples. These results revealed that ORF3 proteins without palmitoylation were not precipitated by ANXA2, consistent with the absence of significant colocalization observed by confocal microscopy (*SI Appendix*, Fig. S7*C*). Collectively, these results demonstrated that palmitoylation of HEV ORF3 at C_{18} and C_{21} is a prerequisite for exercising its function via ANXA2 binding.

ANXA2 Directs ORF3 Sorting into the Vesicles via Association with the Cytoskeleton. ANXA2 is a membrane-associated protein associated with the cytoskeleton (Fig. 5*D*) (18). To determine whether HEV ORF3 is also cytoskeleton-associated, we conducted subcellular fractionation via sequential extraction (33). In addition to the membrane fraction, HEV ORF3 was also detected in the cytoskeletal fraction (Fig. 5*E*). 2-BP treatment reduced the level of ORF3 in the cytoskeletal fraction, suggesting that palmitoylated ORF3 was preferentially transported to the cytoskeleton (Fig. 5*E*). To clarify the role of ANXA2 in directing HEV ORF3 to the cytoskeleton, we analyzed ORF3 distribution in cells depleted of ANXA2 and found that HEV ORF3 was almost undetectable in the cytoskeletal fraction of ANXA2-knockdown cells (Fig. 5*F*). Consistently, the ORF3-C_{18}S/C_{21}S protein, which is incapable of binding to ANXA2, was absent from the cytoskeletal fraction (Fig. 5*F*). Given that HEV ORF3 was found to be sorted into multivesicular bodies (MVBs) for release, and considering that the ORF3-C_{18}S/C_{21}S mutant lost its association with the cytoskeleton, we hypothesized that the ORF3-C_{18}S/C_{21}S mutant may fail to traffic into MVBs. To investigate this, we performed confocal imaging and found that the ORF3 mutant was unable to colocalize with MVB markers, including CD9 and CD63 (Fig. 5*G* and *SI Appendix*, Fig. S7*D*). Based on these results, we propose a model for the egress of HEV ORF3 vesicles and quasi-enveloped virions, where the ORF3 protein is palmitoylated, likely at C_{18} and C_{21}, in the Golgi apparatus or endoplasmic reticulum (*SI Appendix*, Fig. S7 *E* and *F*). Subsequently, palmitoylated ORF3 binds to ANXA2, which is located in the cytoskeleton, and is transported to MVBs for nSMase-ESCRT-mediated sorting. Occasionally, the assembled HEV particles anchor onto the ORF3–ANXA2 complex for budding into the MVB. Ultimately, empty ORF3 vesicles and quasi-enveloped virions are released via the exosomal signaling pathway (Fig. 5*H*).

Mutations at Palmitoylation Sites within ORF3 in Gerbils Abolished HEV Fecal Shedding but with Competent Replication in the Liver. The replication of HEV mutant harboring mutations at palmitoylation sites within ORF3 showed no significant differences compared to the WT virus, as evidenced by ORF2 expression (Fig. 6*A*) and intracellular ORF3 protein levels (Fig. 6*B*); however, the secretion of ORF3 dramatically decreased (Fig. 6*B*). To confirm our findings in vitro and further investigate the role of the ORF3-C_{18}S/C_{21}S mutation in HEV infection in vivo, we intraperitoneally inoculated adult gerbils (13-wk-old) with approximately 10^8 copies of either HEV-WT (n = 15) or HEV-$ORF3_{C18S/C21S}$ (n = 15). Viral RNA was readily detected in the feces of gerbils inoculated with HEV-WT as early as 3 d postinfection, whereas HEV RNA was not detected in the feces of the HEV-$ORF3_{C18S/C21S}$ group (Fig. 6*C*). At 1, 3, 5, and 7 d postinfection, three gerbils from each group were randomly killed, and the liver, kidney, and intestinal tissues were collected. All liver tissues in each group were positive for HEV RNA, at all collection time points, with comparable viral loads, indicating the replication competence of the mutant virus. HEV RNA in the kidney and intestinal tissues collected from both groups of gerbils at 1 d postinfection were positive for HEV RNA. However, starting at 3 d postinfection, HEV RNA was detected less frequently in the kidney and intestinal tissues collected from the mutant group than in the WT group (Fig. 6*D*). Moreover, ORF3 was purified as an exosome from the serum of gerbils infected with HEV-WT, whereas no ORF3 in serum from gerbils infected with HEV-$ORF3_{C18S/C21S}$ was detected (*SI Appendix*, Fig. S8 *A* and *B*). These results suggest that the release of viral particles was blocked by the mutation, thereby reducing the dissemination of virions to extrahepatic tissues. The HEV antigen was also detected in the kidney (Fig. 6*E*), suggesting that the expression of the HEV ORF2 protein in gerbil tissues was unaffected by the mutation. We also assessed the antiviral effects of LCKLSL, an inhibitor of ANXA2 in HEV-infected gerbils. The fecal viral loads of LCKLSL-treated gerbils were lower than those of the control group at 3 d postinfection, but this difference was not observed at 7 d postinfection (Fig. 6*F*). Histological evaluation of liver tissues from infected gerbils 14 d postinfection with HEV-WT

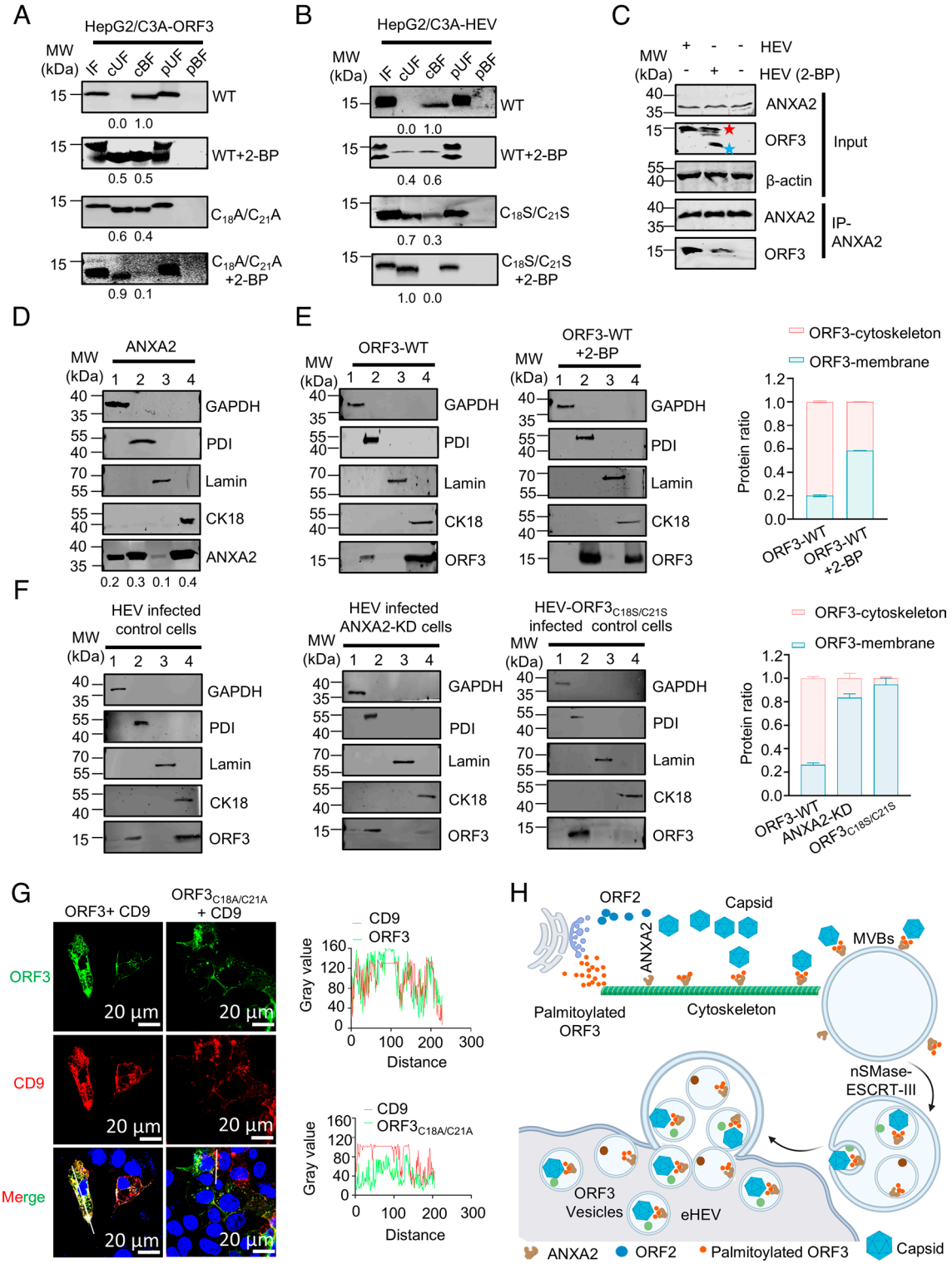

Fig. 5. Palmitoylation of C_{18} and C_{21} is essential for the binding of ORF3 with ANXA2 to anchor the cytoskeleton. (*A* and *B*) A total of 4×10^6 HepG2/C3A cells stably expressing ORF3 or ORF3-C_{18}A/C_{21}A (*A*), or 1.2×10^7 of HepG2/C3A cells infected with HEV (*B*) in the presence or absence of 2-BP were collected for palmitoylation detection. Representative results from two independent experiments are shown. (*C*) HepG2/C3A cells were infected with HEV (genomic copies/cells = 10,000) in the presence or absence of 2-BP (50 μM, 8 h). Cell lysates were collected for coimmunoprecipitation. The blot is representative of two independent experiments. The red entity pentagram indicates palmitoylated ORF3, and blue entity pentagram indicates nonpalmitoylated ORF3. (*D*) Protein fractionation of endogenous ANXA2 in HepG2/C3A cells. Marker proteins of subcellular fractions and ANXA2 were detected by western blotting. The blot is representative of two independent experiments. (*E*) ORF3 protein fractionation in HepG2/C3A cells stably expressing ORF3 in the presence or absence of 50 μM 2-BP; marker proteins of subcellular fractions and ORF3 were detected by western blotting. The protein level of ORF3 associated with cytoskeleton (ORF3-cytoskeleton) or ORF3 associated with membrane (ORF3-membrane) was analyzed by ImageJ. Data represent mean ± SD from three independent experiments, $*P < 0.05$; $**P < 0.01$; $***P < 0.001$; ns, not significant. (*F*) ORF3 protein fractionation in HEV-infected HepG2/C3A cells with or without ANXA2 expression. Marker proteins of subcellular fractions and ORF3 were detected by western blotting. ORF3 protein level associated with cytoskeleton (ORF3-cytoskeleton) or ORF3 associated with membrane (ORF3-membrane) were analyzed by ImageJ. The blot is representative of three independent experiments. (*G*) Confocal microscopy of ORF3 and CD9 in HepG2/C3A cells cotransfected pCAGGS-ORF3-WT/mutant-mWasabi and pCD9-mCherry at 36 h posttransfection. The nucleus was stained with DAPI. Images were captured using a confocal microscope (63×). Fluorescence signals of ORF3 and CD9 were analyzed by ImageJ. (*H*) Model mechanism of secretion of HEV ORF3 vesicles and release of eHEV.

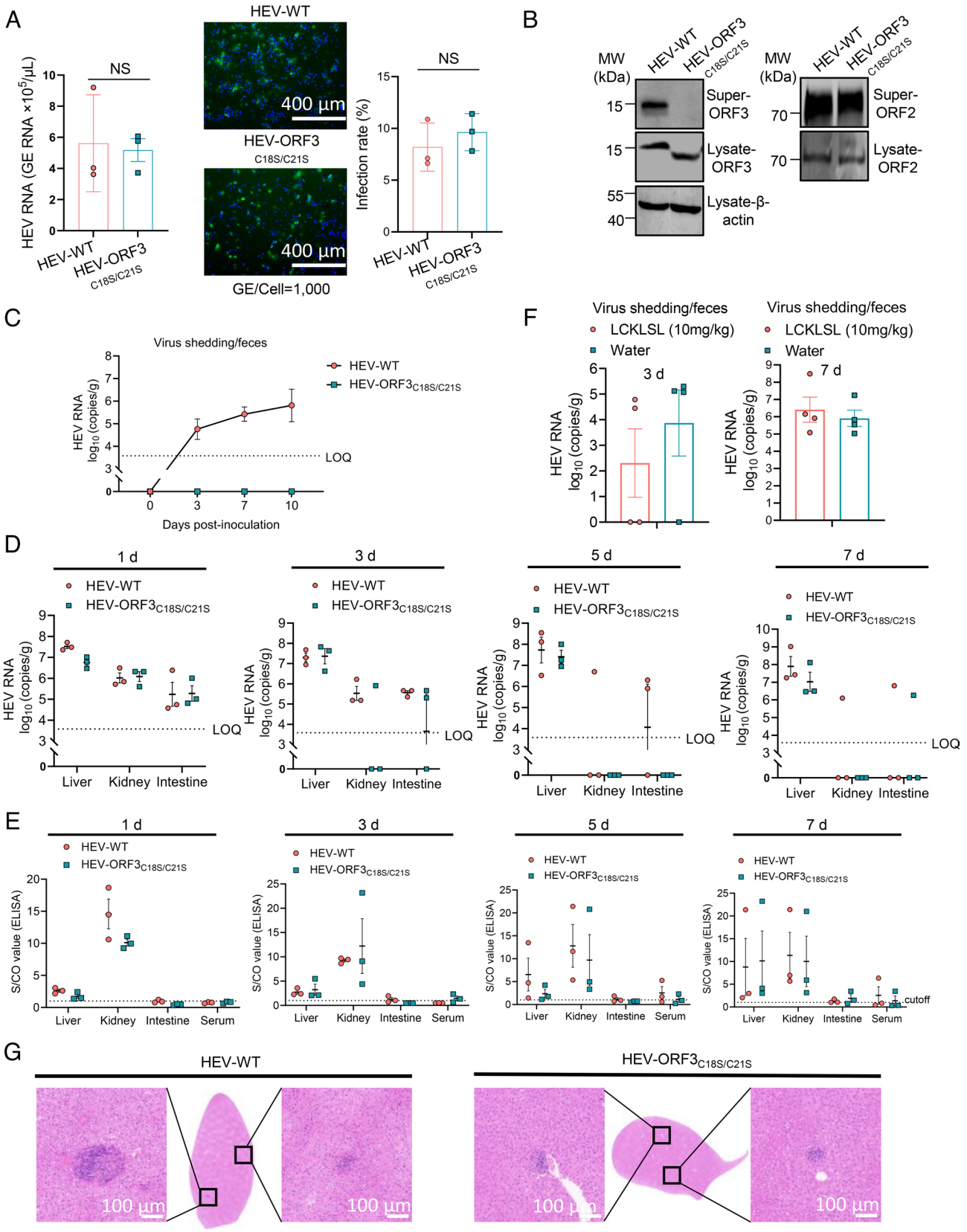

Fig. 6. Infection of HEV-ORF3$_{C18S/C21S}$ in gerbils shows no fecal viral shedding but competent replication in the liver. (*A* and *B*) HepG2/C3A cells were infected with HEV-WT or HEV-ORF3$_{C18S/C21S}$ mutant, and the viral replication was then assessed at 5 d postinfection by detecting intracellular HEV genomic copies by qRT-PCR (*A*), or intracellular and extracellular viral proteins using IFA (*A*) and western blotting (*B*). Data represent mean ± SD from three independent experiments each in duplicate. (*C*–*E*) Gerbils infected with HEV-WT or mutant HEV-ORF3$_{C18S/C21S}$, the viral genomic copies in feces (n = 3) (*C*) or liver, kidney, or intestine (*D*) were detected by qRT-PCR (n = 3); the antigen in the liver, kidney, intestine, or serum was detected by the ELISA (n = 3) at interval days (*E*). (*F*) Gerbils (n = 4) were treated with ANXA2 inhibitor LCKLSL, the viral genomic copies in feces were then detected by qRT-PCR at interval days. Data represent mean ± SEM from four gerbils. (*G*) Representative hematoxylin and eosin (H&E) staining of liver sections from the HEV-WT (1 of 6) and HEV-ORF3$_{C18S/C21S}$-infected (1 of 6) groups 14 d postinfection. The square area of liver tissues presented obvious inflammatory cell infiltration. Scale bars are indicated in the figure.

or the HEV-ORF3$_{C18S/C21S}$ mutant revealed a similar infiltration of lymphocytic inflammatory cells into the portal areas (Fig. 6*G*). Taken together, despite competence in replication, the HEV-ORF3$_{C18S/C21S}$ mutant was unable to release viral particles from hepatocytes, and ANXA2 inhibitors inhibited viral replication in the early period of infection.

Discussion

Based on assembly and morphological criteria, viruses have been categorized into two types: enveloped and nonenveloped viruses (34). eHEV, a quasi-enveloped virion classified in-between nonenveloped and enveloped viruses, is expected to undergo a unique assembly process. Our study reveals that HEV ORF3 plays a crucial role in the assembly and subsequent release of eHEV. It appears that HEV ORF2^{C} proteins first assemble into a pentamer and then into an icosahedral capsid harboring a viral genome akin to naked virions (8). Meanwhile, posttranslationally modified ORF3 proteins in the cytoskeleton capture naked virions and deliver them into MVBs. Ultimately, the assembled quasi-enveloped HEV particles are released via the exosomal pathway. Unexpectedly, we found that partial ORF3 was present in the culture supernatant in a membrane-associated but noninfectious form, suggesting that naked virions may be occasionally captured by ORF3 for subsequent assembly. Further investigation of the underlying mechanisms will shed light on the lifecycle of HEV replication and guide the development of drug and therapeutic strategies.

Palmitoylation plays an important role in the viral lifecycle by regulating trafficking, subcellular localization, and stability of viral proteins (35). For instance, palmitoylation of the SARS-CoV-2 glycoprotein is essential for protein transfer to viral membranes and for viral infectivity (36). Recent findings have revealed that palmitoylation mediates the membrane association of HEV ORF3 and is essential for the secretion of infectious particles (12), however, the underlying mechanism is unclear. Our investigations identified C_{18} and C_{21} as the key sites for palmitoylation of HEV ORF3. Introducing mutations into the HEV genome resulted in an approximately 1.5-log decrease in eHEV release, without affecting intracellular viral replication. Moreover, our findings suggest that inhibition of ORF3 palmitoylation results in the failure of its interaction with ANXA2. ANXA2 knockdown significantly reduced the efficiency of ORF3 and eHEV secretion, highlighting the crucial role of ANXA2 in ORF3 secretion. Numerous studies have reported the role of ANXA2 in viral replication (19–25). ANXA2 interacts with IAV NS1 to promote virion formation and is found on the viral envelope of IAV (21). Additionally, ANXA2 is recruited by HCV NS5A to membrane lipid rafts, facilitating the production of infectious HCV particles (23). Furthermore, ANXA2 promotes BTV release by interacting with viral NS3 protein (25). Surprisingly, all these viral proteins, including IAV NS1, HCV NS5A, and BTV NS3, are predicted to be palmitoylated by the GPS-Palm software. Thus, it would be interesting to explore whether palmitoylation governs the interactions between these viral proteins and ANXA2.

ANXA2 is capable of simultaneously binding to phospholipids and F-actin and is recognized as a cytoskeleton-membrane linking protein (18). ANXA2-knockdown decreased the association of ORF3 with the cytoskeleton. Although ORF3 proteins have been detected in the cytoskeletal fraction previously (11), their significance remains largely unexplored. Here, we report a potential role of ANXA2 as an anchor for the transport of ORF3 on the cytoskeleton, akin to several enveloped viruses whose transfer depends on the host cytoskeleton (20, 37). These observations suggest that the host cytoskeletal elements play an active role in the assembly and budding of viral particles. We found via an extraction assay that ORF3 was enriched in the cytoskeleton fraction, and ANXA2 was hijacked by palmitoylated ORF3 to anchor to the cytoskeleton; however, the precise regulatory mechanism underlying the association between ORF3, ANXA2, and the cytoskeleton requires further study.

Using an HEV infection Mongolian gerbil model, we demonstrated that palmitoylation of ORF3 is necessary for the secretion of infectious particles in vivo. However, HEV replication and ORF2 protein expression can still be detected in liver tissues upon infection with the ORF3 mutant virus in gerbils. HEV RNA detected in the extrahepatic tissues of the ORF3 mutant group in the early stages of infection was possibly due to venous absorption of the virus and ORF2^{S} which were secreted and enriched in kidney tissues. Additionally, ANXA2 inhibitors have been shown to reduce fecal viral loads in the early stages of infection in vivo, indicating a potential future drug and therapeutic strategy.

Viral particles, which are cloaked by the envelope and bound to ORF3, can be detected in the blood of patients infected with HEV, indicating their existence in the form of eHEV (15). Previous studies on HEV-infected cells have shown that eHEV in culture supernatants are also in the form of exosomes (14, 16). In this study, ORF3 was detected by purifying exosomes in the serum of gerbils infected with HEV-WT rather than mutant HEV-ORF3$_{C18S/C21S}$, indicating that ORF3 C_{18} and C_{21} are key sites for the secretion of viral particles and ORF3 vesicles into the serum (*SI Appendix*, Fig. S8*A*). Further studies need to be conducted to explore whether these mutations affect the extrahepatic infection efficiency. To compare the ratio of ORF3 in viral particles and ORF3 vesicles in serum, we performed rate-zonal centrifugation to separate these two entities. Unfortunately, we were unable to purify the ORF3 protein, probably because its content in the serum was too low (*SI Appendix*, Fig. S8*B*).

In summary, we found that not all secreted ORF3 are associated with viral particles. Its secretion requires palmitoylation and recruitment of ANXA2. Binding of ORF3 with ANXA2 anchors ORF3 to the cytoskeleton for transport. During trafficking, ORF3 captures mature viral particles and is secreted as an exosome via the nSMase-ESCRT III pathway. More importantly, palmitoylation of ORF3 and its association with ANXA2 are important for viral fecal shedding and extrahepatic dissemination in the HEV-infected Mongolian gerbil model.

Materials and Methods

Lysates of S10-3 cells transfected with HEV RNA were lysed using three freeze-thaw cycles in distilled water. The virions in the cell lysates were purified by gradient density centrifugation and used to infect cells or gerbils (38) (further details are included in *SI Appendix, Materials and Methods* of virus generation). HepG2/C3A cells (2×10^4) were seeded in flasks coated with rat-tail collagen type 1 (Sigma C3867), and cultured in Dulbecco's Modified Eagle's Medium supplemented with 10% FBS and 2% dimethylsulfoxide at 34.5 °C (9). Adult (13-wk-old) Mongolian gerbils (*Meriones unguiculatus*) were randomly selected and purchased from Sipeifu Biotech (Beijing, China). Each gerbil was inoculated with 500 μL viral stock intraperitoneally (i.p.), with approximately 1×10^8 copies per gerbil. Animals were housed in separate cages with adequate water and food supply. Animal experiments were approved by the Committee of Laboratory Animal Welfare and Ethics, Peking University Health Science Center, and the Committee on the Ethics of Animal Experiments at the Harbin Veterinary Research Institute, Chinese Academy of Agricultural Sciences.

Statistical Analysis. All experiments were performed two or three times, statistical analysis was performed for each experiment, and the data from one independent experiment are shown. The results were analyzed for statistical significance using the Student's *t* test and one-way ANOVA in GraphPad Prism 9.2.0. A *P* value <0.05 was considered statistically significant, and the following categories were

used: *$P < 0.05$, **$P < 0.01$, ***$P < 0.001$, and ****$P < 0.0001$. The detailed procedures are provided in *SI Appendix, Materials and Methods*.

Data, Materials, and Software Availability. All study data are included in the article and/or *SI Appendix*.

ACKNOWLEDGMENTS. This work was supported by the National Natural Science Foundation of China (Grant Number: 32172940) to X.Y., the National Natural Science Foundation of China-Youth Science Fund (Grant Number: 32202888) to X.L., and the National Key Research and Development Program of China (Grant Number: 2023YFC2306900) to L.W.

Author affiliations: [a]Division of Livestock Infectious Diseases, State Key Laboratory for Animal Disease Control and Prevention, Harbin Veterinary Research Institute, Chinese Academy of Agricultural Sciences, Harbin 150069, China; [b]Department of Microbiology and Infectious Disease Center, School of Basic Medical Sciences, Peking University Health Science Center, Beijing 100191, China; [c]Department of Animal Sciences, Quantitative Veterinary Epidemiology Group, Wageningen University, Wageningen 6700 AH, The Netherlands; [d]Center for Vaccines and Immunity, The Research Institute at Nationwide Children's Hospital, Columbus, OH 43205; and [e]Department of Pediatrics, The Ohio State University College of Medicine, Columbus, OH 43205

Author contributions: X.L., Y.-D.T., and X.Y. designed research; X.L., T.L., Z.S., X.X., S.Q., J.G., and M.W. performed research; X.Y. contributed new reagents/analytic tools; X.L., T.L., S.Q., Z.F., L.W., and X.Y. analyzed data; and X.L., T.L., L.W., and X.Y. wrote the paper.

1. S. P. Kenney, The current host range of hepatitis E viruses. *Viruses* **11**, 452 (2019).
2. G. W. Webb, H. R. Dalton, Hepatitis E: An underestimated emerging threat. *Ther. Adv. Infect. Dis.* **6**, 2049936119837162 (2019).
3. P. Hansrivijit *et al.*, Hepatitis E in solid organ transplant recipients: A systematic review and meta-analysis. *World J. Gastroenterol.* **27**, 1240–1254 (2021).
4. M. N. Khaskheli, S. Baloch, A. Sheeba, S. Baloch, Hepatitis E–A preventable health issue-endangering pregnant women's life and foetal outcomes. *J. Pak. Med. Assoc.* **65**, 655–659 (2015).
5. F. Abravanel, S. Lhomme, Hecolin vaccine: Long-term efficacy against HEV for a three-dose regimen. *Lancet* **403**, 782–783 (2024).
6. P. Kar, R. Karna, A review of the diagnosis and management of hepatitis E. *Curr. Treat. Options Infect. Dis.* **12**, 310–320 (2020).
7. S. P. Kenney, X. J. Meng, Hepatitis E virus genome structure and replication strategy. *Cold Spring Harb. Perspect. Med.* **9**, a031724 (2019).
8. T. S. Guu *et al.*, Structure of the hepatitis E virus-like particle suggests mechanisms for virus assembly and receptor binding. *Proc. Natl. Acad. Sci. U.S.A.* **106**, 12992–12997 (2009).
9. X. Yin *et al.*, Origin, antigenicity, and function of a secreted form of ORF2 in hepatitis E virus infection. *Proc. Natl. Acad. Sci. U.S.A.* **115**, 4773–4778 (2018).
10. Q. Ding *et al.*, Hepatitis E virus ORF3 is a functional ion channel required for release of infectious particles. *Proc. Natl. Acad. Sci. U.S.A.* **114**, 1147–1152 (2017).
11. M. Zafrullah, M. H. Ozdener, S. K. Panda, S. Jameel, The ORF3 protein of hepatitis E virus is a phosphoprotein that associates with the cytoskeleton. *J. Virol.* **71**, 9045–9053 (1997).
12. J. Gouttenoire *et al.*, Palmitoylation mediates membrane association of hepatitis E virus ORF3 protein and is required for infectious particle secretion. *PLoS Pathog.* **14**, e1007471 (2018).
13. R. Aggarwal, S. R. Naik, Faecal excretion of hepatitis E virus. *Lancet* **340**, 787 (1992).
14. S. Chapuy-Regaud *et al.*, Characterization of the lipid envelope of exosome encapsulated HEV particles protected from the immune response. *Biochimie* **141**, 70–79 (2017).
15. M. Takahashi *et al.*, Hepatitis E virus (HEV) strains in serum samples can replicate efficiently in cultured cells despite the coexistence of HEV antibodies: Characterization of HEV virions in blood circulation. *J. Clin. Microbiol.* **48**, 1112–1125 (2010).
16. S. Nagashima *et al.*, Characterization of the quasi-enveloped hepatitis E virus particles released by the cellular exosomal pathway. *J. Virol.* **91**, e00822–17 (2017).
17. S. Nagashima *et al.*, Tumour susceptibility gene 101 and the vacuolar protein sorting pathway are required for the release of hepatitis E virions. *J. Gen. Virol.* **92**, 2838–2848 (2011).
18. A. G. Grieve, S. E. Moss, M. J. Hayes, Annexin A2 at the interface of actin and membrane dynamics: A focus on its roles in endocytosis and cell polarization. *Int. J. Cell Biol.* **2012**, 852430 (2012).
19. A. Dziduszko, M. A. Ozbun, Annexin A2 and S100A10 regulate human papillomavirus type 16 entry and intracellular trafficking in human keratinocytes. *J. Virol.* **87**, 7502–7515 (2013).
20. R. Koga, M. Kubota, T. Hashiguchi, Y. Yanagi, S. Ohno, Annexin A2 mediates the localization of measles virus matrix protein at the plasma membrane. *J. Virol.* **92**, e00181–18 (2018).
21. F. LeBouder *et al.*, Annexin II incorporated into influenza virus particles supports virus replication by converting plasminogen into plasmin. *J. Virol.* **82**, 6820–6828 (2008).
22. Q. Zhang *et al.*, ANXA2 facilitates enterovirus 71 infection by interacting with 3D polymerase and PI4KB to assist the assembly of replication organelles. *Virol. Sin.* **36**, 1387–1399 (2021).
23. P. Backes *et al.*, Role of annexin A2 in the production of infectious hepatitis C virus particles. *J. Virol.* **84**, 5775–5789 (2010).
24. C. Sheng *et al.*, Annexin A2 is involved in the production of classical swine fever virus infectious particles. *J. Gen. Virol.* **96**, 1027–1032 (2015).
25. A. R. Beaton, J. Rodriguez, Y. K. Reddy, P. Roy, The membrane trafficking protein calpactin forms a complex with bluetongue virus protein NS3 and mediates virus release. *Proc. Natl. Acad. Sci. U.S.A.* **99**, 13154–13159 (2002).
26. U. Zacharias *et al.*, Ahnak1 abnormally localizes in muscular dystrophies and contributes to muscle vesicle release. *J. Muscle Res. Cell Motil.* **32**, 271–280 (2011).
27. C. Montpellier *et al.*, Hepatitis E virus lifecycle and identification of 3 forms of the ORF2 capsid protein. *Gastroenterology* **154**, 211–223.e8 (2018).
28. K. Yamada *et al.*, ORF3 protein of hepatitis E virus is essential for virion release from infected cells. *J. Gen. Virol.* **90**, 1880–1891 (2009).
29. F. Deng, J. Miller, A review on protein markers of exosome from different bio-resources and the antibodies used for characterization. *J. Histotechnol.* **42**, 226–239 (2019).
30. A. Datta *et al.*, Manumycin A suppresses exosome biogenesis and secretion via targeted inhibition of Ras/Raf/ERK1/2 signaling and hnRNP H1 in castration-resistant prostate cancer cells. *Cancer Lett.* **1**, 73–81 (2017).
31. M. Catalano, L. O'Driscoll, Inhibiting extracellular vesicles formation and release: A review of EV inhibitors. *J. Extracell. Vesicles* **9**, 1703244 (2020).
32. I. A. Aliyu, K. H. Ling, N. Md Hashim, H. Y. Chee, Annexin A2 extracellular translocation and virus interaction: A potential target for antivirus-drug discovery. *Rev. Med. Virol.* **29**, e2038 (2019).
33. H. Vakifahmetoglu-Norberg *et al.*, Caspase-2 promotes cytoskeleton protein degradation during apoptotic cell death. *Cell Death Dis.* **4**, e940 (2013).
34. C. Hepp, N. C. Robb, Coming together during viral assembly. *Nat. Rev. Microbiol.* **16**, 721 (2018).
35. M. E. Linder, R. J. Deschenes, Palmitoylation: Policing protein stability and traffic. *Nat. Rev. Mol. Cell Biol.* **8**, 74–84 (2007).
36. A. A. Ramadan *et al.*, Identification of SARS-CoV-2 spike palmitoylation inhibitors that results in release of attenuated virus with reduced infectivity. *Viruses* **14**, 531 (2022).
37. K. Danastas *et al.*, Herpes simplex virus-1 utilizes the host actin cytoskeleton for its release from axonal growth cones. *PLoS Pathog.* **18**, e1010264 (2022).
38. X. Yin, C. Ambardekar, Y. Lu, Z. Feng, Distinct entry mechanisms for nonenveloped and quasi-enveloped hepatitis E viruses. *J. Virol.* **90**, 4232–4242 (2016).